differential damage to the oocytes/zygotes and 4-cell embryos. One of the special features in SOD1-deficient mice is female infertility (Ho *et al.*, 1998; Matzuk *et al.*, 1998). In this study, 30 oocytes per female were recovered from SOD1-deficient mice after superovulation, and 29.5 oocytes were recovered from wild-type, which implies no difference in the ovulation rate between the two genotypes. We also observed a number of *in vivo*-developed 2-cell embryos from SOD1-deficient mice at 36 h after superovulation and *in vivo*-developed morula and blastocyst 6 embryos at 84–96 h after superovulation (data not shown). At the least, this evidence could ensure *in vivo*-developmental ability of preimplantation embryos in SOD1-deficient female.

In conclusion, we found total 2-cell arrest of embryos from SOD1-deficient mice oocytes in culture under atmospheric oxygen conditions and the negation of the arrest by incubation under hypoxic conditions. Since the mitochondrial function of ATP production via oxidative phosphorylation was almost normal in the embryos, the mechanism of cell cycle regulation might be a target of elevated ROS. After the 4-cell stage, however, embryos suffering from oxidative stress undergo degeneration, most likely by apoptosis. Thus, investigation of embryos developed from SOD1-deficient oocytes would provide a useful clue to an understanding of the mechanisms involved in 2-cell arrest and cellular degeneration at the later developmental stage by intrinsic oxidative stress.

Funding

Partly supported by a grant for Research on Child Health and Development (2005–2008) from the Ministry of Health, Labour and Welfare, Japan, and by the Global COE Program (F03) from the Japan Society for the Promotion of Science (JSPS).

References

Abe H. A non-invasive and sensitive method for measuring cellular respiration with a scanning electrochemical microscopy to evaluate embryo quality. *J Mamm Ova Res* 2007;**24**:70–78.

Acton BM, Jurisicova A, Jurisica I, Casper RF. Alterations in mitochondrial membrane potential during preimplantation stages of mouse and human embryo development. *Mol Hum Reprod* 2004;**10**:23–32.

Agarwal A, Gupta S, Sekhon L, Shah R. Redox considerations in female reproductive function and assisted reproduction: from molecular mechanisms to health implications. *Antioxid Redox Signal* 2008; **10**:1375–1403.

Aitken RJ, Baker MA. Oxidative stress, sperm survival and fertility control. *Mol Cell Endocrinol* 2006;**250**:66–69.

Auerbach S, Brinster RL. Effect of oxygen concentration on the development of two-cell mouse embryos. *Nature* 1968;**217**: 465–466.

Balling R, Haaf H, Maydl R, Metzler M, Beier HM. Oxidative and conjugative metabolism of diethylstilbestrol by rabbit preimplantation embryos. *Dev Biol* 1985;**109**:370–374.

Benos DJ, Balaban RS. Energy requirements of the developing mammalian blastocyst for active ion transport. *Biol Reprod* 1980;**23**:941–947.

Betts DH, Madan P. Permanent embryo arrest: molecular and cellular concepts. *Mol Hum Reprod* 2008;**14**:445–453.

Blander G, de Oliveira RM, Conboy CM, Haigis M, Guarente L. Superoxide dismutase 1 knock-down induces senescence in human fibroblasts. *J Biol Chem* 2003;**278**:38966–38969.

Chatot CL, Lewis JL, Torres I, Ziomek CA. Development of 1-cell embryos from different strains of mice in CZB medium. *Biol Reprod* 1990;**42**:432–440.

Erbach GT, Lawitts JA, Papaioannou VE, Biggers JD. Differential growth of the mouse preimplantation embryo in chemically defined media. *Biol Reprod* 1994;**50**:1027–1033.

Favetta LA, St John EJ, King WA, Betts DH. High levels of p66shc and intracellular ROS in permanently arrested early embryos. *Free Radic Biol Med* 2007;**42**:1201–1210.

Feugang JM, de Roover R, Moens A, Léonard S, Dessy F, Donnay I. Addition of beta-mercaptoethanol or Trolox at the morula/blastocyst stage improves the quality of bovine blastocysts and prevents induction of apoptosis and degeneration by prooxidant agents. *Theriogenology* 2004;**61**:71–90.

Fischer B, Bavister BD. Oxygen tension in the oviduct and uterus of rhesus monkeys, hamsters and rabbits. *J Reprod Fertil* 1993;**99**:673–679.

Fridovich I. Superoxide radical and superoxide dismutases. *Annu Rev Biochem* 1995;**64**:97–112.

Fujii J, Iuchi Y, Okada F. Fundamental roles of reactive oxygen species and protective mechanisms in the female reproductive system. *Reprod Biol Endocrinol* 2005;**3**:43.

Goto Y, Noda Y, Narimoto K, Umaoka Y, Mori T. Oxidative stress on mouse embryo development in vitro. *Free Radic Biol Med* 1992;**13**:47–53.

Halliwell B, Gutteridge JMC. *Free Radical in Biology and Medicine*, 3rd edn. Oxford: Clarendon Press, 1999, 53–55.

Ho YS, Gargano M, Cao J, Bronson RT, Heimler I, Hutz RJ. Reduced fertility in female mice lacking copper-zinc superoxide dismutase. *J Biol Chem* 1998;**273**:7765–7769.

Houghton FD, Thompson JG, Kennedy CJ, Leese HJ. Oxygen consumption and energy metabolism of the early mouse embryo. *Mol Reprod Dev* 1996;**44**:476–485.

Ishii T, Matsuki S, Iuchi Y, Okada F, Toyosaki S, Tomita Y, Ikeda Y, Fujii J. Accelerated impairment of spermatogenic cells in SOD1-knockout mice under heat stress. *Free Radic Res* 2005;**39**:697–705.

Iuchi Y, Okada F, Onuma K, Onoda T, Asao H, Kobayashi M, Fujii J. Elevated oxidative stress in erythrocytes due to an SOD1 deficiency causes anemia and triggers autoantibody production. *Biochem J* 2007; **402**:219–227.

Jinno M, Sandow BA, Hodgen GD. Enhancement of the developmental potential of mouse oocytes matured in vitro by gonadotropins and ethylenediaminetetraacetic acid (EDTA). *J In Vitro Fert Embryo Transf* 1989;**6**:36–40.

Jurisicova A, Acton BM. Deadly decisions: the role of genes regulating programmed cell death in human preimplantation embryo development. *Reproduction* 2004;**128**:281–291.

Keefe DL, Niven-Fairchild T, Powell S, Buradagunta S. Mitochondrial deoxyribonucleic acid deletions in oocytes and reproductive aging in women. *Fertil Steril* 1995;**64**:577–583.

Kitagawa T, Suganuma N, Nawa A, Kikkawa F, Tanaka M, Ozawa T, Tomoda Y. Rapid accumulation of deleted mitochondrial deoxyribonucleic acid in postmenopausal ovaries. *Biol Reprod* 1993; **49**:730–736.

Kuo RC, Baxter GT, Thompson SH, Stricker SA, Patton C, Bonaventura J, Epel D. NO is necessary and sufficient for egg activation at fertilization. *Nature* 2000;**406**:633–636.

Li Y, Huang TT, Carlson EJ, Melov S, Ursell PC, Olson JL, Noble LJ, Yoshimura MP, Berger C, Chan PH *et al.* Dilated cardiomyopathy and neonatal lethality in mutant mice lacking manganese superoxide dismutase. *Nat Genet* 1995;**11**:376–381.

Liu L, Trimarchi JR, Keefe DL. Involvement of mitochondria in oxidative stress-induced cell death in mouse zygotes. *Biol Reprod* 2000; **62**:1745–1753.

Loutradis D, Drakakis P, Kallianidis K, Sofikitis N, Kallipolitis G, Milingos S, Makris N, Michalas S. Biological factors in culture media affecting in vitro fertilization, preimplantation embryo development, and implantation. *Ann N Y Acad Sci* 2000;**900**:325–335.

Matzuk MM, Dionne L, Guo Q, Kumar TR, Lebovitz RM. Ovarian function in superoxide dismutase 1 and 2 knockout mice. *Endocrinology* 1998; **139**:4008–4011.

Nasr-Esfahani MH, Aitken JR, Johnson MH. Hydrogen peroxide levels in mouse oocytes and early cleavage stage embryos developed in vitro or in vivo. *Development* 1990;**109**:501–507.

Natsuyama S, Noda Y, Yamashita M, Nagahama Y, Mori T. Superoxide dismutase and thioredoxin restore defective p34cdc2 kinase activation in mouse two-cell block. *Biochim Biophys Acta* 1993;**1176**: 90–94.

Nishikimi A, Matsukawa T, Hoshino K, Ikeda S, Kira Y, Sato EF, Inoue M, Yamada M. Localization of nitric oxide synthase activity in unfertilized oocytes and fertilized embryos during preimplantation development in mice. *Reproduction* 2001;**122**:957–963.

Noda Y, Matsumoto H, Umaoka Y, Tatsumi K, Kishi J, Mori T. Involvement of superoxide radicals in the mouse two-cell block. *Mol Reprod Dev* 1991;**28**:356–360.

Nonogaki T, Noda Y, Narimoto K, Umaoka Y, Mori T. Effects of superoxide dismutase on mouse in vitro fertilization and embryo culture system. *J Assist Reprod Genet* 1992;**9**:274–280.

Quinn P, Kerin JF, Warnes GM. Improved pregnancy rate in human in vitro fertilization with the use of a medium based on the composition of human tubal fluid. *Fertil Steril* 1985;**44**:493–498.

Ruder EH, Hartman TJ, Blumberg J, Goldman MB. Oxidative stress and antioxidants: exposure and impact on female fertility. *Hum Reprod Update* 2008;**14**:345–357.

Schultz RM. Regulation of zygotic gene activation in the mouse. *BioEssays* 1993;**15**:531–538.

Shiku H, Shiraishi T, Ohya H, Matsue T, Abe H, Hoshi H, Kobayashi M. Oxygen consumption of single bovine embryos probed by scanning electrochemical microscopy. *Anal Chem* 2001;**73**: 3751–3758.

Shiku H, Shiraishi T, Aoyagi S, Utsumi Y, Matsudaira M, Abe H, Hoshi H, Kasai S, Ohya H, Matsue T. Respiration activity of single bovine embryos entrapped in a cone-shaped microwell monitored by scanning electrochemical microscopy. *Anal Biochim Acta* 2004;**522**: 51–58.

Summers MC, Biggers JD. Chemically defined media and the culture of mammalian preimplantation embryos: historical perspective and current issues. *Hum Reprod Update* 2003;**9**:557–582.

Suzuki S, Komatsu S, Kitai H, Endo Y, Iizuka R, Fukasawa T. Analysis of cytoplasmic factors in developmental cleavage of mouse embryo. *Cell Differ* 1988;**24**:133–138.

Suzuki K, Tatsumi H, Satoh S, Senda T, Nakata T, Fujii J, Taniguchi N. Manganese-superoxide dismutase in endothelial cells: localization and mechanism of induction. *Am J Physiol* 1993;**265**:H1173–H1178.

Takahashi M, Keicho K, Takahashi H, Ogawa H, Schultz RM, Okano A. Effect of oxidative stress on development and DNA damage in in-vitro cultured bovine embryos by comet assay. *Theriogenology* 2000;**54**:137–145.

Tarin JJ. Potential effects of age-associated oxidative stress on mammalian oocytes/embryos. *Mol Hum Reprod* 1996;**2**:717–724.

Tarin JJ, Vendrell FJ, Ten J, Cano A. Antioxidant therapy counteracts the disturbing effects of diamide and maternal ageing on meiotic division and chromosomal segregation in mouse oocytes. *Mol Hum Reprod* 1998;**4**:281–288.

Tarin JJ, Perez-Albala S, Cano A. Consequences on offspring of abnormal function in ageing gametes. *Hum Reprod Update* 2000;**6**:532–549.

Tarin JJ, Perez-Albala S, Cano A. Cellular and morphological traits of oocytes retrieved from aging mice after exogenous ovarian stimulation. *Biol Reprod* 2001;**65**:141–150.

Tatone C, Carbone MC, Gallo R, Delle Monache S, Di Cola M, Alesse E, Amicarelli F. Age-associated changes in mouse oocytes during postovulatory in vitro culture: possible role for meiotic kinases and survival factor BCL2. *Biol Reprod* 2006;**74**:395–402.

Telford NA, Watson AJ, Schultz GA. Transcription from maternal to embryonic control in early mammalian development: a comparison of several species. *Mol Reprod Dev* 1990;**26**:90–100.

Thompson JG, Partridge RJ, Houghton FD, Cox CI, Leese HJ. Oxygen uptake and carbohydrate metabolism by in vitro derived bovine embryos. *J Reprod Fertil* 1996;**106**:299–306.

Thouas GA, Trounson AO, Wolvetang EJ, Jones GM. Mitochondrial dysfunction in mouse oocytes results in preimplantation embryo arrest in vitro. *Biol Reprod* 2004;**71**:1936–1942.

Tranguch S, Steuerwald N, Huet-Hudson YM. Nitric oxide synthase production and nitric oxide regulation of preimplantation embryo development. *Biol Reprod* 2003;**68**:1538–1544.

Trimarchi JR, Liu L, Porterfield DM, Smith PJ, Keefe DL. Oxidative phosphorylation-dependent and independent oxygen consumption by individual preimplantation mouse embryos. *Biol Reprod* 2000;**62**:1866–1874.

Valentine JS, Doucette PA, Potter SZ. Copper–zinc superoxide dismutase and amyotrophic lateral sclerosis. *Annu Rev Biochem* 2005;**74**:563–593.

Van Blerkom J. Mitochondria in human oogenesis and preimplantation embryogenesis: engines of metabolism, ionic regulation and developmental competence. *Reproduction* 2004;**128**:269–280.

Van Blerkom J, Davis PW, Lee J. ATP content of human oocytes and developmental potential and outcome after in-vitro fertilization and embryo transfer. *Hum Reprod* 1995;**10**:415–424.

Wilhelm J, Vytásek R, Ostádalová I, Vajner L. Evaluation of different methods detecting intracellular generation of free radicals. *Mol Cell Biochem* 2009;**328**:167–176.

Journal of Reproduction and Development, Vol. 56, No. 2, 2010

—Technology Report—

Viability of Porcine Embryos after Vitrification Using Water-soluble Pullulan Films

Nobutada SAKAGAMI[1)], Tadashi YAMAMOTO[1)], Kiyoshi AKIYAMA[1)], Yoshinori NAKAZAWA[1)], Nobuo KOJIMA[1)], Kouji NISHIDA[1)], Shoko YOKOMIZO[2)], Yuji TAKAGI[2)], Hiroyuki ABE[3)], Chie SUZUKI[4)] and Koji YOSHIOKA[4)]

[1)]Kanagawa Prefectural Livestock Industry Technology Center, Ebina 243-0417, [2)]Faculty of Agriculture, Shinshu University, Minamiminowa 399-4598, [3)]Graduate School of Science and Engineering, Yamagata University, Yonezawa 992-8510 and [4)]National Institute of Animal Health, Tsukuba 305-0856, Japan

Abstract. The efficiency of a porcine embryo vitrification method that uses water-soluble films of pullulan, a naturally-occurring polysaccharide polymer, was compared with two other types of vitrification methods using different devices and solutions for vitrification and warming. Blastocysts collected *in vivo* and vitrified by the conventional straw (ST), Cryotop® (MVC) or pullulan film vitrification (PFV) methods were stored in liquid nitrogen for a certain period of time, after which the cryoprotective agents were removed by stepwise dilution. Fresh embryos were used as controls for the non-vitrification group. The vitrified-warmed embryos were incubated in TCM199 with 0.1 mM β-mercaptoethanol and 20% fetal bovine serum for 24 h at 38.5 C in humidified air with 5% CO_2 to evaluate their viability. The survival rate of embryos in the ST group (48.3%) was significantly lower than that of those in the MVC (70.7%), PFV (79.0%) and non-vitrification (94.4%) groups. The oxygen consumption rate after vitrification was significantly lower than that before vitrification in the ST group, but was not significantly different in the MVC and PFV groups. Both the oxygen consumption rates of embryos after warming and the live cell numbers in the ST group were lower than those in the MVC group, while they did not differ significantly between the PFV and MVC groups. There was a correlation between the oxygen consumption rate and the number of live cells in vitrified embryos after warming. Our results demonstrated that *in vivo*-derived porcine embryos could be vitrified using pullulan films.

Key words: Oxygen consumption rate, Porcine embryo, Pullulan film, Vitrification

(J. Reprod. Dev. 56: 279–284, 2010)

Preservation of porcine embryos is important for increasing the effective use of high-quality genetic resources, preventing disease transmission via animals and allowing low-cost transportation of pigs. Due to the extremely high sensitivity of porcine embryos to low temperature, it has been difficult with slow freezing methods to achieve conception rates and litter sizes equivalent to those achieved with artificial insemination [1, 2]. However, it has recently become possible to produce piglets from cryopreserved embryos by using ultra-rapid vitrification methods, such as the minimum volume cooling (MVC) [3, 4], open pulled straw [5], microdroplet [6] and metal mesh vitrification [7] methods.

Pullulan, which is a neutral polysaccharide polymer also known as α-1,4-; α-1,6-glucan, is made from starch and consists of maltotriose units linked in an orderly manner. It has been reported that murine morulae placed on a pullulan film could be vitrified [8]. In general, stepwise dilution is required after warming of vitrified embryos, since vitrification requires a high concentration of cryoprotective agents (CPAs), which makes it difficult, due to their toxicity, to warm the embryos in a straw for direct transfer to recipients. As the pullulan film is soluble in warm water, the vitrification solution can be diluted in a straw, and then the embryos can be directly transferred into a recipient using a straw-attached intrauterine injector.

Several studies on non-surgical embryo transfer in pigs have been reported [9–13], and we have also been working on the development of a non-surgical transfer technique that uses a straw-attached intrauterine injector [14]. Direct transfer via a straw containing vitrified embryos with high viability may be applied to piglet production by non-surgical embryo transfer in an ordinary commercial farm.

Measuring the oxygen consumption rate using a scanning electrochemical microscope may be effective as a non-invasive evaluation of embryo quality [15]. We have previously reported that bovine embryos having a high oxygen consumption rate showed a high conception rate after embryo transfer [16]. In an attempt at embryo cryopreservation using the slow-freezing method, the oxygen consumption rate in embryos significantly decreased after freezing and thawing, indicating that the embryos were damaged by the cryopreservation procedure [16]. However, there are no reports available concerning the oxygen consumption rate before and after cryopreservation with *in vivo*-derived porcine embryos.

In the present study, to investigate the potential for application of the pullulan film vitrification (PFV) method in a non-surgical transfer technique for porcine embryos, we compared the survival rate of porcine embryos preserved by the PFV method with those attained by conventional vitrification methods. We also measured

Received: June 11, 2009
Accepted: November 18, 2009
Published online in J-STAGE: December 25, 2009

Correspondence: N Sakagami (e-mail: sakagami.semi@pref.kanagawa.jp)

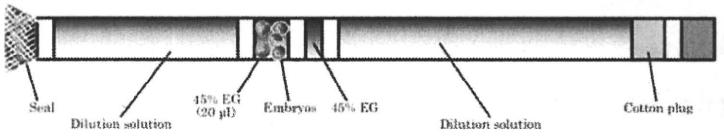

Fig. 1. A straw containing four liquid layers: (from the cotton-plug side) a dilution solution (PB1 + 1.7 M galactose + 0.5% BSA), a 45% EG vitrification solution (PB1 + 45% EG + 7% PVP + 0.5% BSA) that prevents reduction in the concentration of the vitrification solution due to mixing with the diluents of the first layers, a 45% EG vitrification solution containing embryos and a dilution solution. The straw was sealed after being filled with the last dilution layer.

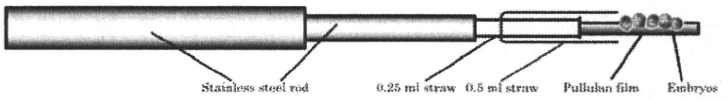

Fig. 2. A stainless steel rod for vitrification equipped with a pullulan film. A stainless steel rod was attached to a short 0.25-ml straw, and a pullulan film was attached to the tip of the straw. The 0.25-ml straw and pullulan film were covered with a case made from a 0.5-ml straw. Embryos and vitrification solution were placed on the pullulan film, and after the embryos were vitrified in liquid nitrogen, the case was slid across to cover the film.

the oxygen consumption rate of embryos before and after vitrification to examine how the rate was influenced by these vitrification methods.

Materials and Methods

Embryo collection from gilts

All animal-related procedures followed in this study were done with the approval of the Institutional Animal Experiment Committee of Kanagawa Prefectural Agriculture Facilities. A total of 39 prepubertal gilts (Landrace and Large White, 5.5–7.3 months old) were used for collection of embryos, as previously described with some modifications [13]. Briefly, superovulation was induced by intramuscular injection of 1500 IU eCG (Peamex, Sankyo, Tokyo, Japan), followed 72 h later by 500 IU hCG (Puberogen, Sankyo). The gilts were artificially inseminated twice, in the afternoon one day after hCG injection and in the morning two days after hCG injection.

In the morning on Day 6 (Day 0=the day of the first artificial insemination), the embryos were recovered from the uterine horns by laparotomy under general anesthesia (4–5% [v/v] halothane) by flushing with PB1 [17] with 0.5% (w/v) bovine serum albumin (BSA; Fraction V, Sigma Chemical, St. Louis, MO, USA) or TALP-Hepes [18]. The recovered embryos were morphologically evaluated under an inverted microscope (× 100), and only blastocysts were used for the experiments. The blastocysts were preserved in PZM-5 [10] supplemented with 10% (v/v) fetal bovine serum (FBS; Gibco, Life Technologies, Grand Island, NY, USA) at 38.5 C in humidified air with 5% CO_2 until vitrification.

Vitrification and warming of embryos

The embryos were vitrified using the three different methods and warmed 20–150 days later.

In Method 1, conventional vitrification using a mini-straw (ST) was performed using 0.25-ml crystal straws (IMV Technologies, L'Aigle, France) as described previously [19] with some modifications. Briefly, the embryos were placed in a drop (80 μl) of equilibration solution consisting of PB1 medium with 11% (v/v) ethylene glycol (EG) and 0.5% BSA (11% EG solution) for 5 min at room temperature (20–25 C). After equilibration in 11% EG solution, the embryos were transferred to a vitrification solution consisting of PB1 medium supplemented with 45% EG, 7% (w/v) polyvinylpyrrolidone (MW 10,000, Sigma) and 0.5% BSA (45% EG vitrification solution) preloaded into a straw. Within 40 sec of the initial exposure of the embryos to the 45% EG vitrification solution, the straw was loaded with the solutions, as shown in Fig. 1, heat sealed and placed on a styrene foam board (5 mm thick) floating on liquid nitrogen (LN_2), and the cotton-plug part of the straw was dipped into LN_2 for a quick moment to create ice seeds in the diluent. The straw was then placed on the styrene foam board again for 3 min. After confirming that the 45% EG vitrification solution was transparent and that ice crystals had not been formed, the straw was plunged into LN_2.

After storage in LN_2 for a certain period of time, the straw was warmed in air (25 C) for 5 sec and then in a 40 C water bath for 6 sec. Immediately after warming, the straw was shaken to mix the solutions inside (i.e., first-step dilution). Two minutes after the first-step dilution, the content of the straw was expelled into a dish, and the embryos were subsequently washed by five serial transfer steps of the warmed embryos in PB1 medium supplemented with 0.5% BSA and 6%, 3%, 1.4%, 0.7% or 0% EG for 2 min each.

In Method 2, the MVC method was conducted using a Cryotop® and commercial vitrification and warming solutions (VT101 and VT102, Kitazato BioPharma, Shizuoka, Japan) by the method previously reported [3, 4]. The embryos were contracted by dehydration in an equilibration solution (ES of VT101, Kitazato BioPharma) and kept at room temperature (25 C) for 5 to 10 min until they regained their volume to some extent. The equilibrated

embryos were transferred to a vitrification solution (VS of VT101, Kitazato BioPharma) along with a minimal amount of the equilibration solution. The embryos contracted in the solution were loaded onto the tip of a Cryotop® and directly plunged into LN_2. The length of time from exposure of the embryos to the vitrification solution until storage in LN_2 was less than 60 sec.

After storage in LN_2, the embryos were warmed by immersing the Cryotop® tip into a warming solution (TS of VT102, Kitazato BioPharma) at 38.5 C. After one min, the embryos were transferred to a diluent (DS of VT102, Kitazato BioPharma) at 38.5 C for 3 min and then washed twice in a washing solution (WS of VT102, Kitazato BioPharma) for 5 min each time.

In Method 3, the PFV method was conducted using a pullulan film (1.5 mm wide, 15 mm long and 20 μm thick; Hayashibara Shoji, Okayama, Japan) attached to a stainless steel rod (Fig. 2). The embryos were kept in D-PBS with 20% FBS for 2 min, equilibrated for 4 min in D-PBS with 20% FBS supplemented with 7.5% EG, 7.5% DMSO and 0.3 M sucrose and then transferred to a vitrification solution (EDS30; D-PBS with 15% EG, 15% DMSO, 0.6 M sucrose and 20% FBS). Within 60 sec after transfer to the vitrification solution, the embryos were loaded onto the pullulan film and plunged into LN_2.

After storage in LN_2, the embryos were warmed by submerging the film successively into D-PBS supplemented with 20% FBS and 0.6 M sucrose for 2 min, D-PBS supplemented with 20% FBS and 0.3 M sucrose for 2 min and finally D-PBS with 20% FBS for 2 min.

Viability of embryos

Following warming, the embryos were cultured in TCM199 supplemented with 0.1 mM β-mercaptoethanol and 20% FBS for 24 h at 38.5 C in humidified air with 5% CO_2. The embryos forming a blastocoel were considered viable. As the non-vitrification control, embryos just recovered were also cultured for 24 h in the same medium.

Measurement of the oxygen consumption rate

The oxygen consumption rate using an embryo respirometer (HV-403, Research Institute for the Functional Peptides, Yamagata, Japan), a device developed based on a scanning electrochemical microscope, was measured for some of the embryos 30 min before vitrification and after warming by the method of Abe *et al.* [15]. Briefly, an embryo was placed into the solution for the measurement (ERAM-2, Research Institute for the Functional Peptides) on the flat bottom of a cone-shaped microwell on the plate (RAP-1, Research Institute for the Functional Peptides). A microelectrode (platinum microelectrode RAE-1, Research Institute for the Functional Peptides) was moved close to the embryo, and a voltage of –0.6 V was applied to reduce the oxygen concentration in the solution surrounding the embryo and measure the current generated as a result. The oxygen concentration gradients in the solution surrounding the embryo were measured by scanning the z-axis (i.e., horizontal direction) at a speed of 31.0 μm/sec. The average of two measurements (anterior and posterior sides of the embryo) was considered to be the oxygen consumption rate of the embryo.

Table 1. *In vitro* development of porcine embryos cryopreserved by different vitrification methods

Vitrification method	No. of embryos	
	Cultured	Survived (%)
ST	89	43 (48.3)[a]
MVC	82	58 (70.7)[b]
PFV	81	64 (79.0)[b]
Non-vitrification	54	51 (94.4)[c]

[a–c] Values with different superscripts within each column are significantly different ($P<0.05$).

Classification of viable and dead cells in embryos

The method of Saha and Suzuki [20] was used to compare the cell viability of the vitrified embryos. After washing with TCM199 containing 20% FBS, the embryos subjected to oxygen consumption rate measurement were warmed to 38.5 C and cultured in a staining solution for 30 min for double staining of viable and dead cells. TCM199 supplemented with 10 μg/ml bisbenzimide (Hoechst 33342, Calbiochem, San Diego, CA, USA) and 10 μg/ml propidium iodide (PI; Sigma) was used as the staining solution. The stained embryos were washed with TCM199 containing 20% FBS, placed on a slide with a small amount of TCM199 with 20% FBS and covered with a cover glass. The embryos were observed through a U-MWU filter (excitation wavelength of 365 nm, barrier filter of 400 nm) under an inverted microscope equipped with a fluorescent light source, and embryos with blue nuclei were counted as viable; those with pink nuclei were counted as dead.

Statistical analysis

The experiment was repeated three or four times for each group. A chi-square test and Fisher's exact probability test was used to compare the viability of embryos. The numbers of cells were subjected to logarithmic transformation before statistical analysis. An analysis of variance (ANOVA) was performed using the General Linear Model (GLM) procedure of SPSS (SPSS 11.5J, User's Guide, SPSS, Tokyo, Japan) followed by the Scheffe test. Linear relationships and correlation coefficients between oxygen consumption rate and the number of live cells in vitrified-warmed embryos were determined by simple regression analysis and Pearson correlation coefficient analysis, respectively. A P value of less than 0.05 was considered statistically significant.

Results

Effect of vitrification procedures on morphological changes in vitrified embryos after warming

The viabilities of embryos after vitrification and warming by the different methods are shown in Table 1. The percentage of embryos that survived in the ST group was significantly lower ($P<0.05$) than those in the other two vitrification groups and in the non-vitrification group. There was no significant difference in the rates between the MVC and PFV groups. Moreover, the survival rate in the non-vitrification group was significantly higher ($P<0.05$) than those in the other groups.

Table 2. Oxygen consumption rates of porcine embryos before and after vitrification

Vitrification method	No. of embryos examined	Oxygen consumption rate (F × 10^{14} /mol s^{-1})	
		Before vitrification	After warming*
ST	10	1.29 ± 0.17^{A}	$0.82 \pm 0.09^{a,B}$
MVC	15	1.15 ± 0.08	1.22 ± 0.08^{b}
PFV	11	0.99 ± 0.08	1.02 ± 0.09^{ab}
Non-vitrification	10	1.32 ± 0.14	–

Mean ± SEM. * Values were measured 30 min after warming. ^{a,b} Values with different superscripts within each column are significantly different (P<0.05). ^{A,B} Values with different superscripts within each row are significantly different (P<0.05).

Table 3. Cell viability of porcine embryos after vitrification

Vitrification method	No. of embryos examined	Mean cell no. in blastocyst		Ratio of live /total (%)
		Total	Live	
ST	10	70.0 ± 2.5	64.4 ± 3.2^{a}	91.9 ± 2.7^{a}
MVC	13	86.2 ± 4.3	85.9 ± 4.4^{b}	99.5 ± 0.3^{b}
PFV	9	82.3 ± 3.5	80.2 ± 4.3^{ab}	97.0 ± 1.8^{ab}
Non-vitrification	10	70.3 ± 3.7	70.3 ± 3.7^{ab}	100 ± 0^{b}

Mean ± SEM. ^{a,b} Values with different superscripts within each column are significantly different (P<0.05).

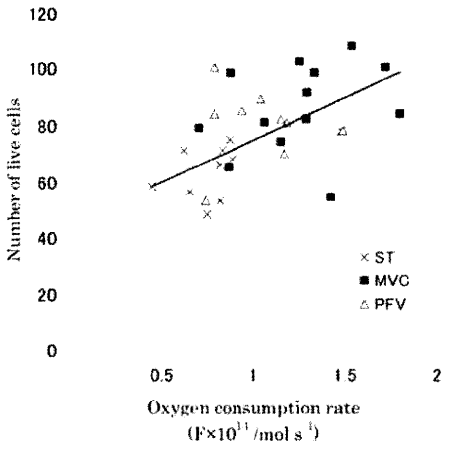

Fig. 3. Correlation between the oxygen consumption rates of vitrified-warmed embryos and number of live cells. There is a significant positive correlation between the oxygen consumption rate and the number of live cells (P<0.01 r=0.496). Regression lines are drawn to show the relationship between the oxygen consumption rates and numbers of live cells.

Effect of vitrification procedures on the oxygen consumption rates of embryos

The oxygen consumption rate of the vitrified embryos after warming was significantly higher in the MVC group (P<0.05) than in the ST group, but in the PFV group, it did not differ significantly from the rates in the other groups (Table 2). The oxygen consumption rate after warming was significantly lower (P<0.05) than that at pre-vitrification in the ST group, while there was no significant difference between these rates in the MVC and PFV groups.

Effect of vitrification procedures on cell viability in embryos

Cell viability after vitrification by the different methods is shown in Table 3. The ratio of live to total cell number was significantly lower (P<0.05) in the ST groups than in the MVC and non-vitrification groups. There was a positive correlation between the oxygen consumption rate and the number of live cells (P<0.01, r = 0.496) in all vitrified-warmed embryos (Fig. 3).

Discussion

The present study demonstrated that porcine blastocysts can be vitrified using a pullulan film and that viability, oxygen consumption rate and cell viability were not different from those of embryos vitrified by the MVC method using a Cryotop®.

Since vitrification uses CPAs at high concentrations to prevent intracellular ice crystal formation, their toxicity causes damage to embryos when the vitrification procedure takes a long time. To avoid this problem, several vitrification methods, such as the open-pulled straw [5], microdroplet [6] and metal mesh vitrification [7] methods, have been reported to achieve high viability by making porcine embryos very rapidly pass a critical temperature range at which embryos are injured. The viability of embryos is increased by these methods, as they have the advantages of minimizing the required amounts of CPAs by using special devises and lowering the concentration of CPAs by application of rapid cooling. The present study compared the viability of embryos in the PFV method using pullulan film with that in the MVC method, one of the ultra-rapid vitrification methods, and demonstrated that the viability was 70% or more in the PFV method, which is similar to that in the MVC method. On the other hand, the survival rate of embryos in

the ST group was significantly lower than that in the other groups. The volume of vitrification solution was smaller in the MVC and PFV groups (0.1 μl) than in the ST group (20 μl). Moreover, whereas embryos were placed into LN_2 after exposing them to LN_2 vapor in the ST group, they were directly plunged into LN_2 in the MVC and PFV groups. Thus, the difference in survival may be due to a more rapid temperature decrease in the MVC and PFV groups than in the ST group.

The vitrification procedure for embryo storage does not require a programmable freezer. However, it requires special devises and strict control of temperature and time before plunging the embryos into LN_2 because high concentrations of CPAs are used. Therefore, the number of embryos that can be vitrified in one operation has been limited. Ushijima *et al.* [4] reported that the MVC method allows simultaneous vitrification of 8 to 12 embryos. In pigs, it is desirable to cryopreserve larger numbers of embryos together because 15 to 20 embryos should be transferred into a recipient at one time. In the present study, 5 to 8 embryos could be simultaneously vitrified by using a sheet of pullulan film, and the vitrified embryos on 3 or 4 sheets of the film could be loaded together into a straw. We suggest that the PFV method to cryopreserve porcine embryos is a valuable tool for non-surgical embryo transfer in pigs, since the vitrified embryos can be directly transferred into a recipient. We have obtained normal calves after transfer of bovine blastocysts vitrified using pullulan films and warmed by one-step dilution in straws (our unpublished data). The PFV method appeared to have no adverse effect on porcine embryos in this study. If porcine embryos vitrified using pullulan films can be conveniently diluted and warmed in a straw while maintaining their viability, they may be applied to piglet production by non-surgical embryo transfer under on-farm conditions. Further technical improvements are required to enable one-step dilution in a straw.

In the present study, PFV was applied as an open method in which the solution containing embryos directly contacts LN_2. Storage of embryos in open containers in LN_2 may represent an increased potential for microbial contamination during long-term banking and the risk of disease transmission by embryo transfer [21]. To avoid contamination of pathogens, embryos collected from the same donor should be separately vitrified by the PFV method in its own sterile LN_2 and stored in its own closed containers. An in-straw dilution method after PFV may also enable decrease of the risk of contamination because storage and dilution of vitrified embryos is performed in a sealed straw.

The oxygen consumption rate of embryos vitrified by the three different methods was measured in order to assess the quality of embryos and their potential use in a non-invasive transfer method [16, 22, 23]. To our knowledge, the present study is the first to measure the oxygen consumption rate before and after vitrification of porcine embryos. The oxygen consumption rate after warming was significantly lower than the pre-vitrification levels in the ST group, while there was no significant difference between these rates in the MVC and PFV groups, thus reflecting their respective viabilities. These results were consistent with the viabilities of the embryos after vitrification and warming in these groups, supporting the validity of using the oxygen consumption rate as an index of embryo quality after vitrification and warming.

Dobrinsky *et al.* [24] have reported that success of vitrification depends on the influence of CPAs on morphological and molecular properties of cellular organelles and membranes. In the present study, cell damage of embryos was assessed by a double staining method with Hoechst 33342 and PI, which can distinguish between blue-stained live cells and pink-stained dead cells by the difference in permeability for PI, depending on damage of the cell membrane. The number of live cells in the ST group decreased significantly compared with the MVC group ($P<0.05$), and the ratio of live to total cells was reduced by 5 to 7% in the ST group compared with the other groups. This result may reflect that the survival rate of embryos after warming was markedly lower in the ST group (48.3%) than in the MVC (70.7%), PFV (79.0%) and non-vitrified groups (94.4%). Moreover, both the oxygen consumption rates of embryos just after warming and live cell numbers in the MVC group were higher than those in the ST group. In addition, there was a correlation between the oxygen consumption rate and the number of live cells in vitrified embryos after warming. Trimarchi *et al.* [22] have demonstrated that maturation of mitochondria correlates with an increase in metabolic activity, as reflected in the oxygen consumption rate, and that the oxygen consumption rate reflects the number of cells measured and their mitochondrial activity. Thus, we assumed that the number of live cells could be estimated by the oxygen consumption rate.

In the present study, no difference was found in viability and oxygen consumption rate after warming between the porcine embryos vitrified by the method using pullulan film and those obtained by the previously reported MVC method, indicating that porcine embryos can be vitrified using pullulan film. Non-surgical direct transfer of ultra-rapidly vitrified porcine embryos without using a microscope would be a useful transfer method applicable by individual farmers in the field. Therefore, further studies are desirable on the method for in-straw dilution of embryos.

Acknowledgments

The authors would like to thank Drs H Hoshi and K Misumi for critical suggestions and T Wada, Y Shimizu, H Ozawa, T Kashiwagi, K Tani and H Ayabe for technical assisitance. This study was supported by grants for "Research for the Utilization and Industrialization of Agricultural Biotechnology" (1605) from the Ministry of Agriculture, Forestry and Fisheries of Japan and the "Research and Development Program for New Bio-Industry Initiatives" from the Bio-oriented Technology Research Advancement Institution (BRAIN).

References

1. **Polge C, Wilmut I, Rowson LEA.** The low temperature preservation of cow, sheep and pig embryos. *Cryobiology* 1974; 11: 560.
2. **Pollard JW, Leibo SP.** Chilling sensitivity of mammalian embryos. *Theriogenology* 1994; 41: 101–106.
3. **Esaki R, Ueda H, Kurome M, Hirakawa K, Tomii R, Yoshioka H, Ushijima H, Kuwayama M, Nagashima H.** Cryopreservation of porcine embryos derived from *in vitro*-matured oocytes. *Biol Reprod* 2004; 71: 432–437.
4. **Ushijima H, Yoshioka H, Esaki R, Takahashi K, Kuwayama M, Nakane T, Nagashima H.** Improved survival of vitrified *in vivo*-derived porcine embryos. *J Reprod Dev* 2004; 50: 481–486.

5. **Cuello C, Gil MA, Parrilla I, Tornel J, Vázquez JM, Roca J, Berthelot F, Martinat-Botté F, Martínez EA.** *In vitro* development following one-step dilution of OPS-vitrified porcine blastocysts. *Theriogenology* 2004 ; 62: 1144–1152.
6. **Misumi K, Suzuki M, Sato S, Saito N.** Successful production of piglets derived from vitrified morulae and early blastocysts using a microdroplet method. *Theriogenology* 2003; 60: 253–260.
7. **Fujino Y, Kojima T, Nakamura Y, Kobayashi H, Kikuchi K, Funahashi H.** Metal mesh vitrification (MMV) method for cryopreservation of porcine embryos. *Theriogenology* 2008; 70: 809–817.
8. **Takagi Y, Shimizu M, Kato T, Danguri A, Sakamoto M.** Vitrification of mouse morulae by a new method: pullulan film-straw vitrification. *Reprod Fertil Dev* 2004; 16: 183 (abstract).
9. **Yonemura I, Fujino Y, Irie S, Miura Y.** Transcervical transfer of porcine embryos under practical conditions. *J Reprod Dev* 1996; 42: 89–94.
10. **Suzuki C, Iwamura S, Yoshioka K.** Birth of piglets through the non-surgical transfer of blastocysts produced *in vitro*. *J Reprod Dev* 2004; 50: 487–491.
11. **Martinez EA, Caamaño JN, Gil MA, Rieke A, McCauley TC, Cantley TC, Vazquez JM, Roca J, Vazquez JL, Didion BA, Murphy CN, Prather RS, Day BN.** Successful nonsurgical deep uterine embryo transfer in pigs. *Theriogenology* 2004; 61: 137–146.
12. **Cuello C, Berthelot F, Martinat-Botté F, Venturi E, Guillouet P, Vázquez JM, Roca J, Martínez EA.** Piglets born after non-surgical deep intrauterine transfer of vitrified blastocysts in gilts. *Anim Reprod Sci* 2005; 85: 275–286.
13. **Nakazawa Y, Misawa H, Fujino Y, Tajima S, Misumi K, Ueda J, Nakamura Y, Shibata T, Hirayama Y, Kikuchi K.** Effect of volume of non-surgical embryo transfer medium on ability of porcine embryos to survive to term. *J Reprod Dev* 2008; 54: 30–34.
14. **Fujino Y, Nakamura Y, Kobayashi H, Nakano S, Suzuki C, Yoshioka K.** Viability of porcine embryos vitrified by the metal mesh vitrification method after surgical or non-surgical transfer. *Reprod Fertil Dev* 2007; 19: 221–222 (abstract).
15. **Abe H, Shiku H, Aoyagi S, Hoshi H.** *In vitro* culture and evaluation of embryos for production of high quality bovine embryos. *J Mamm Ova Res* 2004; 21: 22–30.
16. **Sakagami N, Akiyama K, Nakazawa Y.** The relationship between oxygen consumption rate and pregnancy rate of bovine embryos. *Reprod Fertil Dev* 2007; 19: 225 (abstract).
17. **Quinn P, Barros C, Whittingham DG.** Preservation of hamster oocytes to assay the fertilizing capacity of human spermatozoa. *J Reprod Fertil* 1982; 66: 161–168.
18. **Bavister BD, Leibfried ML, Lieberman G.** Development of preimplantation embryos of the golden hamster in a defined culture medium. *Biol Reprod* 1983; 28: 235–247.
19. **Kobayashi S, Takei M, Kano M, Tomita M, Leibo SP.** Piglets produced by transfer of vitrified porcine embryos after stepwise dilution of cryoprotectants. *Cryobiology* 1998; 36: 20–31.
20. **Saha S, Suzuki T.** Vitrification of *in vitro* produced bovine embryos at different ages using one- and three-step addition of cryoprotective additives. *Reprod Fertil Dev* 1997; 9: 741–746.
21. **Bielanski A, Bergeron H, Lau PCK, Devenish J.** Microbial contamination of embryos and semen during long term banking in liquid nitrogen. *Cryobiology* 2003; 46: 146–152.
22. **Trimarchi JR, Liu L, Porterfield DM, Smith PJS, Keefe DL.** Oxidative phosphorylation-dependent and -independent oxygen consumption by individual preimplantation mouse embryos. *Biol Reprod* 2000; 62: 1866-1874.
23. **Lopes AS, Madsen SE, Ramsing NB, Løvendahl P, Greve T, Callesen H.** Investigation of respiration of individual bovine embryos produced *in vivo* and *in vitro* and correlation with viability following transfer. *Hum Reprod* 2007; 22: 558–566.
24. **Dobrinsky JR.** Cellular approach to cryopreservation of embryos. *Theriogenology* 1996; 45: 17–26.

日本受精着床学会雑誌 27(1) 53-58, 2010

電気化学的呼吸計測技術におけるヒト胚クオリティー評価と安全性

Evaluating the Safety and Quality of Human Embryos with Measurement of Oxygen Consumption by Scanning Electrochemical Microscopy

後藤 香里[1]　小池　恵[1]　熊迫 陽子[1]
宇津宮隆史[1]　荒木 康久[2]　阿部 宏之[3]

Kaori Goto[1], Megumi Koike[1], Yoko Kumasako[1],
Takafumi Utsunomiya[1], Yasuhisa Araki[2], Hiroyuki Abe[3]

[1]*St-Luke Clinic, 5, Tsumori Tomioka, Oita City, Oita 870-0947, Japan*
[2]*The Institute for ARMT, 909-21, Ooaza Ishii, Setagun Fujimi, Gunma 391-0105, Japan*
[3]*Graduate School of Science and Engineering, Yamagata University, 4-3-16, Jyonan, Yonezawa City, Yamagata 992-8510, Japan*

要旨：プローブ電極を用いた走査型電気化学顕微鏡(SECM)は，局所領域における生物反応を電気化学的にモニタリングできる。本研究では，電気化学呼吸計測技術を応用したヒト胚クオリティー評価法の安全性と胚評価の可能性を検討した。体外受精－胚移植または凍結胚移植を施行した後の未移植胚に対し，個々の胚の透明帯近傍をマイクロ電極で走査し胚の酸素消費量を測定した。測定時の最適状態を保つため，顕微鏡に設置されている保温プレートの温度について検討した。呼吸量測定群と非測定群にて胚の胚盤胞発生率も比較した。測定群は51.8%であり非測定群は57.0%と差は認めなかった。測定時のDay 3における分割は4細胞期～10細胞期であったが，平均呼吸量は各分割期で偏りはみられず，また，Veeckの分類とは相関のない呼吸活性を示した。測定後の胚を培養した結果，呼吸量が0.26–0.56 × 10^{-14}/mol·s^{-1}であった胚の胚盤胞発生率は65.8%であり，0.26未満または0.56より大きい場合の胚盤胞発生率は39%と有意差が認められた。SECMを用いて胚の呼吸活性を計測することにより，従来のVeeck分類では知りえなかった胚の質を安全により厳密に評価することができる可能性が示唆された。

キーワード：呼吸量，走査型電気顕微鏡，安全性，胚評価，ヒト胚

ABSTRACT: Respiration is a useful parameter for evaluating embryo quality as it provides important information about metabolic activity. A scanning electrochemical microscopy (SECM) measuement system provides a non-invasive, simple, accurate, and consistent measurement of the respiration activity of single human embryos. In this study, we describe an accurate method for assessing the quality of individual human embryos. We measured oxygen consumption rates of human embryos at various cleavage stages. We monitored the temperature of the hot plate which was installed in the microscope to keep the most suitable state at the time of the measurement. We compared the blastocyst development of embryos in the measurement group with those of the no-measurement group. The measured embryos (51.8%) showed the same developmental rate to the blastocyst as the no-measurement group embryos (57.0%). There were no significant differences in the mean rates of oxygen consumption at each cleavage stage. Embryos with moderate respiration rates (0.26–0.56 × 10^{-14}/mol·s^{-1}) showed a high developmental rate (65.8%) to the blastocyst. The developmental rate of embryos with lower and higher respiration rates (<0.26 × 10^{-14}/mol·s^{-1} and >0.56 × 10^{-14}/mol·s^{-1}) was 39.0%. These results support the suggestion that measuring embryonic respiration provides safety and valuable information about embryo quality.

Key words: Respiration, scanning electrochemical microscopy, safety, evaluation of embryos, human embryo

受付日：2009年7月1日／受理日：2009年11月30日

[1]セント・ルカ産婦人科　〒870-0947　大分県大分市津守富岡5組
TEL: 097-568-6060　FAX: 097-568-6299
e-mail: lukelab@oct-net.ne.jp
[2]高度生殖医療技術研究所，[3]山形大学大学院理工学研究科物質化学工学専攻

緒　言

現在，体外受精における移植胚の選択は，移植時の胚の形態を主に行っている。妊娠率の向上，多胎率，流産率を減少させるには，より着床しうる能力を持った胚を

選択することが不可欠である。現在，胚のクオリティー評価は簡単で非侵襲的な方法である形態評価法が最も普及している。しかし，形態評価法は観察者の主観により判定結果に差が生じる可能性があるため，より客観的で，精度が高く，安全な胚クオリティー評価法の開発が望まれている。

著者らは形態観察に比べてより客観的な方法として，細胞呼吸能測定による胚クオリティー評価方法を提案している。これは，高感度で生体反応を検出できる電気化学的計測技術の基盤である走査型電気化学顕微鏡（SECM）を用いて非侵襲的に胚の呼吸量を測定し，呼吸能を指標に胚のクオリティーを評価する新しい方法である。これまでにウシ胚を用いた研究により，呼吸活性を基盤とする胚クオリティー評価法の開発に成功している[1,2]。さらに，SECMを用いて単一のヒト胚の呼吸量測定に初めて成功した[3]。そこで本研究は，SECMを用いた胚の評価が安全でかつ着床能を有する胚の選択が可能となるかを検討するために，まず胚の発育を観察した。Day 3胚（体外受精＝Day 0）の呼吸量を測定後，追加培養を行い，呼吸量測定胚と非測定胚の発育能を比較することで，胚への影響を調査した。胚呼吸量の違いと胚発育の関係についても検討した。また，物理的影響を避けるため，最適顕微鏡ステージ温度についても検討を行った。

方　法

患者背景および測定方法

体外受精胚移植または凍結胚移植を施行し，患者の同意が得られた未移植胚を研究に用いた。対象期間は2006年7月から2007年7月で73周期188個の胚を測定した。平均年齢は34.5 ± 4.5歳で平均体外受精施行回数は2.7 ± 2.3回だった。受精後1日から3日までは，Sydney IVF Cleavage Medium（Cook社）を用いて5% O_2, 6% CO_2, 90% N_2の気相下に37℃で培養を行った。受精日をDay 0とし，Day 3にて4～10細胞期胚に発生した胚をVeeckの分類法[4]を基に評価した。胚を形態観察により評価した後，SECMをベースに開発した「受精卵呼吸測定装置」を用いて個々の胚の呼吸量を測定した。呼吸測定後，胚発生能を調べるために個々の胚をSydney IVF Blastocyst medium（Cook社）に培養液の交換を行い，Day 5–7まで培養した。装置は，倒立型顕微鏡，ポテンショスタット，呼吸解析ソフトを内蔵したノートパソコンにより構成されている。呼吸量の測定には，マイクロ電極と参照電極，測定プレートを用いた。測定プレートに10% Synthetic serum substitude（SSS；IS Japan）を添加したmodified-Human Follicle Fluid（m-HFF；扶桑薬品工業株式会社）を5 ml入れ，マイクロウェルの中にミネラルオイルが混入しないように胚を洗浄した後，マイクロウェルの底部中心に胚を静置した。参照電極を測定プレートの端に設置した後，マイクロ電極を透明帯の間近に移動させた。ポテンショスタットの電位を－0.6 V vs. Ag/AgCl（参照電極）に保持した後，移動速度30 μm/sec，走査距離160 μmの条件で透明帯に対して鉛直方向（Z軸方向）に掃引した（図1）。1個の胚に対する測定時間は約30秒である。測定中のマイクロウェル内温度や浸透圧変化を最小に留めるため，最適顕微鏡ステージ温度の検討を行った。浸透圧測定にはOSMOSTAT（アークレイ株式会社）を用い測定を行った。

結　果

顕微鏡ステージ温度について検討を行った。経時的に温度と浸透圧変化を調べた（図2）。40度に顕微鏡ステージ温度を設定した場合20分以後より温度低下を示し，45度では5分後より温度の上昇を認めた。浸透圧変化では，45度に設定した場合15分後には290 mOsm/kgを上回り上昇が早くなる結果を示した。42.5度では培養液の液温も35度を保ち浸透圧も30分までは300 mOsm/kgを上回ることはなく，比較的最適な条件を長く保つことが可能であると考えられる。

呼吸量測定による，胚発育への影響を評価するために呼吸量測定群と呼吸量非測定群で胚盤胞発生率も比較した。呼吸量測定群で胚盤胞発生率は57.0%，非測定群で51.8%と差は認めなかった（図3）。

同一分割期において，それぞれの胚の呼吸能に顕著な違いが認められた。例えば，Veeckの分類によって4分割グレード1と形態的に同じクオリティーと評価された胚の呼吸量を比較した結果，呼吸測定値はそれぞれ①0.25，②0.44，6分割グレード2では③0.57，④0.23，8分割グレード2では⑤0.71，⑥0.35であり胚によって顕著な違いが認められた（図4）。このように本研究では，Veeckの分類法による形態的評価と胚の呼吸能には明確な相関は認められなかった。Day 3における4～10細胞期胚(n=187)の呼吸量を測定した。各分割期の酸素消費（呼吸）量を表1に示す。呼吸量（$F \times 10^{14}$/mol s^{-1}）の平均値は，0.34–0.50であり各分割期間に顕著な差はなかった。Day 3胚の呼吸量測定後，胚盤胞期まで培養し，呼吸能と胚盤胞発生率の関係を調べた。その結果，Day 3において呼吸量が0.26-0.56 × 10^{14}/mol s^{-1}であった胚は65.8%が胚盤胞に発生した。一方，呼吸量が0.26 × 10^{14}/mol s^{-1}未満及び0.56 × 10^{14}/mol s^{-1}より大きい場合の胚盤胞発生率は，39.0%であった（図5）。

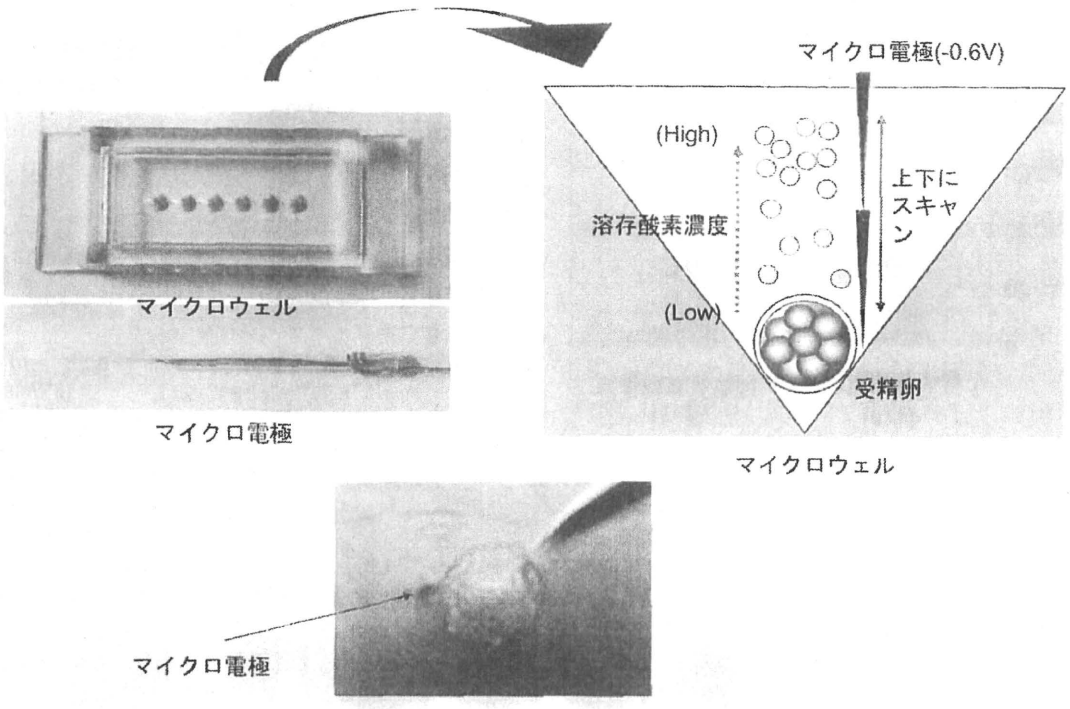

図1　SECMを用いた呼吸量測定

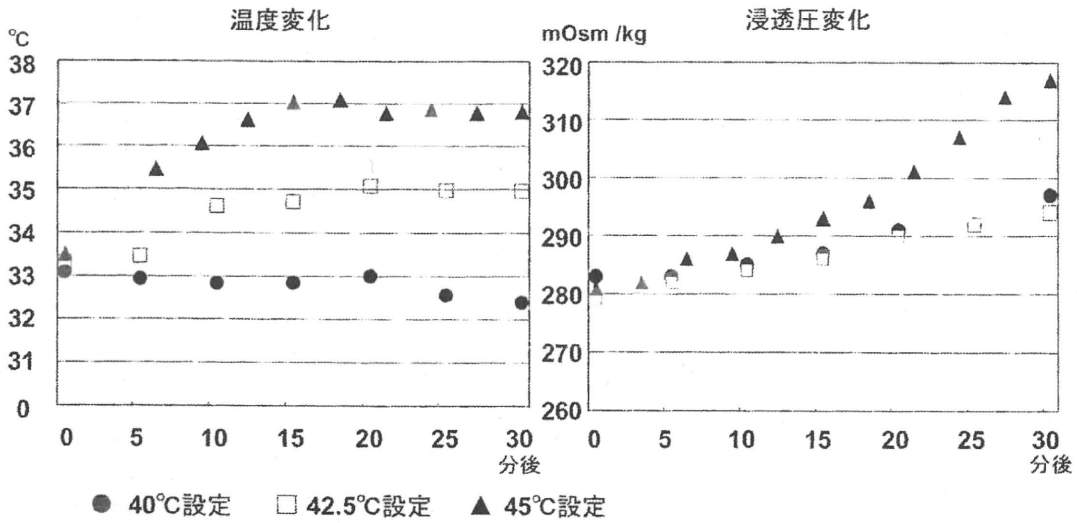

図2　顕微鏡ステージ温度における培養液変化

考　察

胚移植にあたり，最も良好な胚を選別し，1個の移植をすることは多胎率の低下のために不可欠である。これまで，分割期胚の段階でクオリティー良好胚を選別するための形態的判断基準として多くの施設でVeeckの分類[4]が使用されている。さらに，よりクオリティー良好な胚を選択するために様々な判定基準について研究が進められてきた。Zollnerら[5]は前核の接着や前核数の評価に基づく，スコアリングシステムを開発・提案している。

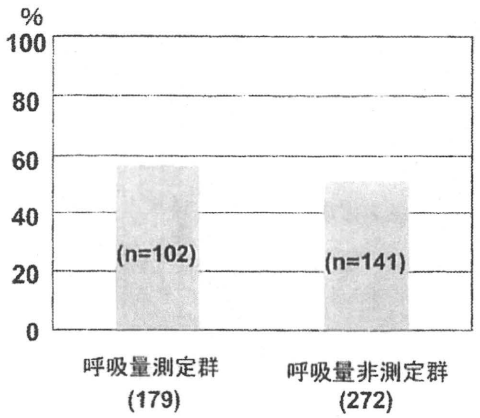

図3　呼吸量測定，非測定群における胚盤胞発生率

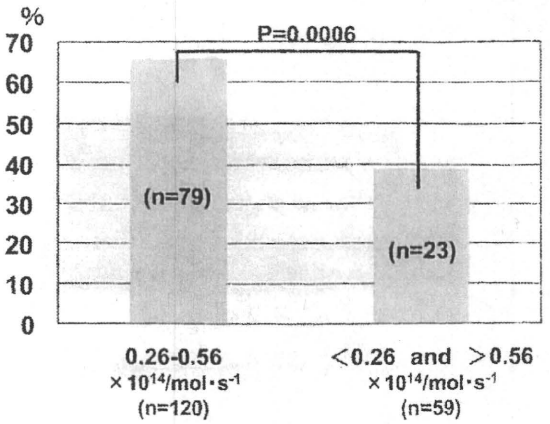

図5　ヒト胚の呼吸能と胚盤胞発生率の関係

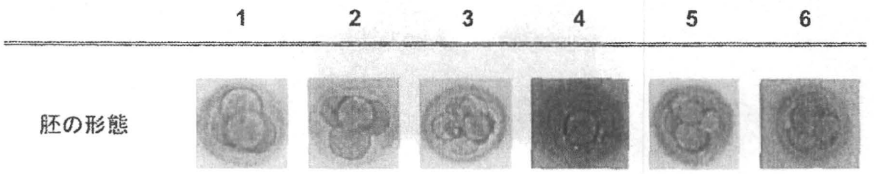

Veeck法による評価	4分割 グレード1	4分割 グレード1	6分割 グレード2	6分割 グレード2	8分割 グレード2	8分割 グレード2
胚呼吸量 ($F\times10^{14}$/mol·s^{-1})	0.25	0.44	0.57	0.23	0.71	0.35

図4　ヒト体外受精胚の形態と呼吸量

表1　異なる分割期におけるヒト胚の酸素消費量（呼吸量）

分割期	測定胚数	呼吸量 ($F\times10^{14}$/mol·s^{-1})
4細胞	8	0.34 ± 0.1
5細胞	15	0.45 ± 0.2
6細胞	39	0.37 ± 0.1
7細胞	51	0.39 ± 0.2
8細胞	50	0.40 ± 0.2
9細胞	12	0.40 ± 0.1
10細胞	12	0.50 ± 0.2

N.S

Scottら[6]，Tesarik and Greco[7]や公文ら[8]は，前核や核小体の形態による判定を提案している。また，Cirayら[9]は，2細胞期のそれぞれの細胞の核の局在の判定と早期分割による胚発生能の評価法を提案している。しかし，いずれも形態的特徴の観察による評価法であるため，判定結果が観察者の主観によって影響を受ける可能性は否定できない。1998年頃からは，培養期間が長くなることにより移植胚の選別が容易になると考えられ，胚盤胞期移植が広まった。しかし，一卵性双胎が増加することや，培養期間が長くなるため，胚移植キャンセルになる可能性が高くなるという欠点も持ち合わせている。そのため，大多数の施設ではDay 2もしくはDay 3の分割期胚を移植しているのが現状である。分割期胚移植と胚盤胞移植の比較検討としては，Gardnerら[10]やScholtesら[11]が，胚

胚盤胞移植を行うことにより，妊娠率は分割期胚移植に比べて有意に上昇したと報告をしている。しかし，Coskunら[12]，Karakiら[13]やUtsunomiyaら[14]により，胚盤胞まで発育が進まず移植キャンセルとなった症例を含めた上での妊娠率は分割期胚移植と有意差はないという報告もなされている。分割期胚移植の検討としては，受精確認からDay 2移植もしくはDay 3移植の妊娠率の比較を行った結果，Carilloら[15]の妊娠率に差があるという報告の一方，Lavergeら[16]は妊娠率に差はないという報告をした。

阿部らは，胚のクオリティーに関連する微細構造の解析を行い，ミトコンドリアが胚のクオリティーに密接に関係していることを発見している[17]。ミトコンドリアは酸化的リン酸化反応（呼吸）により細胞活動に必要なエネルギー（ATP）を産生することから，ミトコンドリアが発達している胚は呼吸活性が高く，一方の不良胚ではミトコンドリアの呼吸代謝能が低いと考えられる。この研究成果を基に阿部らは，高感度・非侵襲的に細胞の呼吸を検出できる電気化学計測技術に着目し，この計測技術の中心であるSECMをベースとする受精卵呼吸測定装置を開発した[1, 18, 19]。これまでに，ウシ，ブタ，マウスの胚の無侵襲的呼吸能解析に成功しており，呼吸能を指標とする胚クオリティー評価法の有効性を示している[2]。最近，電気化学的呼吸計測技術のヒト胚への応用を目的に，ヒト余剰胚の呼吸量測定を行っている。体外受精後の全ての発生ステージにおいて胚の呼吸量測定に成功するとともに，ミトコンドリアの発達と呼吸量の増加が一致することを明らかにした[3]。また，以前に我々はヒト胚の形態と呼吸能との関連性を調べた結果，胚の呼吸能とVeeckの分類法による形態的評価は必ずしも一致することはないことを示し，電気化学計測法は，形態観察では評価できない胚の呼吸能をモニタする可能性を報告した[20]。

今回我々はこの呼吸計測技術が胚へ及ぼす影響を調査するとともに胚評価の可能性についても検討を行った。呼吸量計測に用いるマイクロ電極はピコアンペアレベルの電流の変化を検出できる。この微小電極の周りに生じる電場は電圧が0.1 μV以下，電流は1 nA以下であり，細胞の膜電位（60-90 mv）の60万分の1以下のため胚への影響は無いと思われる。測定時の温度や浸透圧変化を考え測定プレートを保温する顕微鏡ステージの最適温度についても検討した。40度，42.5度，45度で検討を行ったが，40度では測定プレート内温度の低下が見られ，45度では温度に問題はないものの，浸透圧の上昇が早くなった。m-HFFの指示する浸透圧は275–295 mOsm/kgである。そこで我々は42.5度に設定し呼吸量測定を行った。1個の胚に対し測定に要する時間は30秒だが，マイクロ電極を胚の透明帯近傍に静置すること，次の胚へ電極を移動する動作も含めると1個の胚への所要時間は1分以内である。また，1回の測定で測る胚の個数も少数に制限している。呼吸測定を行った胚への影響は胚盤胞の発生率を以って評価したが，呼吸量測定群，非測定群で差は認められなかった。

胚呼吸量と胚発育の関係では呼吸量0.26–0.56を示す胚で胚盤胞発生率がそれ以外と比較して高くなる結果を示した。これはミトコンドリアによる呼吸活性と胚のクオリティーが密接に関係している可能性がある。呼吸量が0.26より低い胚は胚盤胞への発育が低い。これはミトコンドリアにおける活性が低いことを示しており，胚発育へ影響を与えていることが考えられる。呼吸量が0.56より高い胚でも胚盤胞への発育が低い。阿部らはクオリティー良好胚では，受精胚から胚盤胞期にかけて多くのミトコンドリアにおいてサイズの増加やクリステの拡張が認められ，呼吸量が増加していくことを報告している[21]。このことから，胚発育が低い原因としてDay 3時の早い時期にミトコンドリアが発達し過ぎていることも考えられ，胚盤胞へ到達する前に活性が終息してしまうかもしれない。その結果，呼吸活性が低すぎても高すぎても胚盤胞発育が低くなる結果を示したのではないかと思われる。

本研究では，電気化学的呼吸測定技術を応用した新しいヒト胚クオリティー評価の安全性と可能性が示された。胚の呼吸測定と形態的評価を併用することで，より厳密に胚のクオリティーを評価できる可能性がある。今後は妊娠率を含めた臨床的有用性を検討していく必要があると思われる。

文　献

1) Abe, H., Shiku, H., Aoyagi, S., Hoshi, H.: In vitro culture and evaluation of embryos for production of high quality bovine embryos. J Mamm Ova Res., 21: 22-30, 2004.
2) Abe, H., Shiku, H., Yokoo, M., Aoyagi, S., Moriyasu, S., Minamihashi, A., Matsue, T., Hoshi, H.: Evaluating the quality of individual embryos with a non-invasive and highly sensitive measurement of oxygen consumption by scanning electrochemical microscopy. J Reprod Dev., 52 (Suppl): S55–S64, 2006.
3) 阿部宏之・横尾正樹・荒木康久・他：電気化学的イメージング法を応用した単一ヒト胚の呼吸能解析．産婦人科の実際 56: 2053–2057, 2007.
4) Veeck, L.L.: Atlas of the human oocyte and early conceptus. Vol. 2. Williams & Wilkins, Baltimore, 1991.
5) Zollner, U., Zollner, K.P., Hartl, G., Dietl, J., Steck, T.: The use of a detailed zygote score after IVF/ICSI to obtain good quality blastocysts: the German experience. Hum. Reprod., 17: 1327-1333, 2002.

6) Scott, L., Alvero, R., Leondires, M., Miller, B.: The morphology of human pronuclear embryos is positively related to blastocyst development and implantation. Hum Reprod., 15: 2394–2403, 2000.
7) Tesarik, J., Greco, E.: The probability of abnormal preimplantation development can be predicted by a single static observation on pronuclear stage morphology. Hum. Reprod., 14: 1318–1323, 1999.
8) 公文麻美・大中英子・長木元孝・他：前核期胚における形態的評価の検討，第58回日本不妊学会九州支部会抄録集，2001.
9) Ciray, H.N., Karaqenc, L., Uluq, U., Bener, F., Bahceci, M.: Early cleavage morphology affects the quality and implantation potential of day 3 embryos. Fertil. Steril., 85: 358–365, 2006.
10) Gardner, D.K., Schoolcraft, W.B., Wargley, L., Schlenker, T., Stevens, J., Hesla, J.: A prospective randomized trial of blastocyst culture and transfer in in-vitro fertilization. Fertil. Steril., 13: 3434–3440, 1998.
11) Scholtes, M.C., Zeilmaker, G.H.: Blastocyst transfer in day-5 embryo transfer depends primarily on the number of oocytes retrieved and not on age. Fertil. Steril., 69: 78–83, 1998.
12) Coskun, S., Hollanders, J., Al-Hassan, S., Al-Sufyan, H., Al-Mayman, H., Jaroud, K.: Day-5 versus day-3 embryo transfer; a controlled randomized trial. Hum. Reprod., 15: 1947–1952, 2000.
13) Karaki, R.Z., Samarraie, S.S., Younis, N.A., Lahloub, T.M., Ibrahim, M.H.: Blastocyst culture and transfer; a step toward improved in vitro fertilization outcome. Fertil. Steril., 77: 114–118, 2002.
14) Utsunomiya, T., Ito, H., Nagaki, M., Sato, J.: A Prospective, Randomized Study: Day-3 versus Hatching Blastocyst Stage. Hum. Reprod., 19: 1598–1603, 2004.
15) Carrillo, A.J., Lane, B., Pridham, D.D., Risch, P.P., Pool, T.B., Silverman, I.H., Cook, C.L.: Improved clinical outcomes for in vitro fertilization with delay of embryo transfer from 48 to 72 hours after oocyte retrieval; use of glucose- and phosphate-free media. Fertil. Steril., 69: 329–334, 1998.
16) Laverge, H., De Sutter, P., Van der Elst, J., Dhont, M.: A prospective , randomized study comparing day 2 and day 3 embryo transfer in human IVF. Hum. Reprod., 16: 476–480, 2001.
17) Abe, H., Matsuzaki, S., Hoshi, H.: Ultrastructural differences in bovine morulae classified as high and low qualities by morphological evaluation. Theriogenology, 57: 1273–1283, 2002.
18) Shiku, H., Shiraishi, T., Ohya, H., Matsue, T., Abe, H., Hoshi, H., Kobayashi, M.: Oxygen consumption of single bovine embryos probed with scanning electrochemical microscopy. Anal Chem,73: 3751–3758, 2001.
19) Shiku, H., Shiraishi, T., Aoyagi, S., Utsumi, Y., Matsudaira, M., Abe, H., Hoshi, H., Kasai, S., Ohya, H., Matsue, T.: Respiration activity of single bovine embryos entrapped in a cone-shaped microwell monitored by scanning electrochemical microscopy. Anal Chim Acta, 522: 51–58, 2004.
20) 那須　恵・後藤香里・熊迫陽子・宇津宮隆史・荒木康久・橋尾正樹・阿部宏之：電気化学的呼吸計測によるヒト胚のクオリティー評価，産婦人科の実際，57: 289–294, 2008.
21) 阿部宏之：電気化学的イメージング技術を応用した胚のクオリティー評価，産婦人科の実際，55: 207–216, 2006.

Journal of Biomechanical Science and Engineering

Vol. 5, No. 3, 2010

Biomechanical Contribution of Cytoskeletal Structures to Traction Forces in Cultured Smooth Muscle Cells*

Toshiro OHASHI**, Norifumi KAMEDA***, Shouji NAKAMURA**** and Masaaki SATO*****

** Department of Bioengineering and Robotics, Graduate School of Engineering, Tohoku University, 6-6-01 Aoba-yama, Sendai 980-8579, Japan (Present: Hokkaido University, Japan)
E-mail: ohashi@bml.mech.tohoku.ac.jp (Present: ohashi@eng.hokudai.ac.jp)

*** Department of Bioengineering and Robotics, Graduate School of Engineering, Tohoku University, 6-6-01 Aoba-yama, Sendai 980-8579, Japan (Present: Yokohama Rubber Co., Ltd, Japan)

**** Department of Bioengineering and Robotics, Graduate School of Engineering, Tohoku University, 6-6-01 Aoba-yama, Sendai 980-8579, Japan (Present: HOYA Corporation, Japan)

***** Department of Bioengineering and Robotics, Graduate School of Engineering/Department of Biomedical Engineering, Graduate School of Biomedical Engineering, Tohoku University, 6-6-01 Aoba-yama, Sendai 980-8579, Japan

Abstract

Cellular traction forces were measured by using a microfabricated substrate, particularly exploring how cytoskeletal structures such as actin filaments and microtubules contribute to traction forces. Smooth muscle cells isolated from bovine aortas were cultured and transfected with fluorescence proteins to visualize cell microstructures and then plated on a micropatterned elastomer substrate with arrays of micropillars. Cell spreading on the substrates produced deflection of micropillars which was used for estimation of cellular traction forces, and was closely associated with organization of stress fibers of actin filaments. Traction forces varied considerably among cells, showing the order of several 10 nN. After disruption of microtubules with nocodazole, traction forces significantly increased and there was no detectable change in formation of stress fibers. To inhibit the ROCK pathway, a signaling pathway of myosin light chain phosphorylation, possibly being induced by disruption of microtubules, significantly depressed the increase in traction forces after the disruption of microtubules. This result indicates that microtubules disassembly may regulate the actomyosin-based contractile system mainly through the ROCK pathway. The present study suggests that formation of stress fibers are mainly involved in cellular traction forces and a contribution of microtubules should include not only a force balance but also rather a modulator of the actomyosin contractile system in actin stress fibers.

Key words: Traction Forces, Stress Fibers, Microtubules, Actomyosin Force Generation, Intracellular Stress Balance

1. Introduction

It is well known that cells adhere to their extracellular matrix at focal adhesions, generating traction forces. Focal adhesions are therefore the primary sites at which forces are transmitted from/to the extracellular matrix. Cellular traction forces are believed to play an important role in the interactions between cells and their

*Received 10 Sep., 2009 (No. 09-0503)
[DOI: 10.1299/jbse.5.262]

substrates, possibly involving many cellular functions such as migration, proliferation and cell remodeling [1,2].

So far, many studies have been performed to estimate cellular traction forces using microfabrication techniques. Balaban et al. [3] have utilized a combined method of micropatterning of elastomer substrates and fluorescence imaging of focal adhesions in live cells expressing GFP-tagged vinculin to explore the molecular mechanism underlying the regulation of cell adhesion. They showed that local forces have a correlation with orientation, fluorescence intensity and area of the focal adhesions. They also characterized the dynamics of the force-dependent modulation of the focal adhesions by blocking actomyosin contractility, indicating a relaxation of force. Tan et al. [4] have measured cellular traction forces for the first time by using microfabricated arrays of elastomeric, microneedle-like posts. They controlled the geometry of the posts and showed that cell morphology regulates the magnitude of traction force.

It is believed that cellular traction forces may be attributable to the actomyosin-based contractile system and physically coupling integrins to contractile actin filaments are thus important element to transmit traction forces to extracellular matrix. Ingber [5] has proposed cellular tensegrity model assuming the whole cell a prestressed tensegrity model. In the model, actin filaments and intermediate filaments contribute to tensional forces, and these forces are balanced by microtubules that resist compression and extracellular matrix adhesions. However, this model is still controversial. Although efforts have been made to estimate cellular traction forces with implications for mechanical role of cytoskeletal structures, little is still known of how cytoskeletal structures contribute to cellular traction forces. Previous reports have studied the effect of microtubule disruption on an increase in traction forces relating to mechanical role of actin filament structure [6,7,8]. One possible idea to explain this increase may be that tensional forces generated by actin filaments are balanced by microtubules that resist compression. An alternative explanation is that disruption of microtubules may be attributable mainly to activation of the contractile machinery. However, whether the microtubule contributions involved are given mechanically or biochemically, and if biochemically what is the pathway are not fully understood.

In this study, we estimate cellular traction forces of smooth muscle cells by using a microfabricated substrate with arrays of micropillars to further address fundamental aspects of how cytoskeletal structures contribute to smooth muscle cell mechanics. In particular, focusing on implication in activation of actomyosin contractility, inhibition of signaling pathways of myosin light chain phosphorylation is for the first time combined with cellular traction force experiments to explore biochemical contribution of microtubules disassembly to contraction of stress fibers.

2. Materials and Methods

2.1 Cell culture

Smooth muscle cells from bovine thoracic aortas were purchased (Cell Applications, Inc., CA, USA). The cells were seeded in tissue culture flasks with Dulbecco's modified Eagle medium (DMEM, Gibco, MD, USA) supplemented with 10% heat-inactivated fetal bovine serum (JRH Biosciences, KS, USA), penicillin and streptomycin (Gibco). Cells were grown in a 37°C humidified atmosphere of 95% air and 5% CO_2 gas. Cells were confluent after 4-5 days and then passaged at a 1:4 split ratio in the flasks using trypsin-EDTA. Cultured cells

181

from the 4th to 9th generation were studied. This culture procedure can lead to the modulation of smooth muscle cells from a contractile to a synthetic phenotype characteristic.

2.2 Gene transfection and fluorescence observation

Prior to experiments, a plasmid vector encoding GFP (green fluorescent protein) fused to the amino terminus of actin and fused to the alpha-tubulin (BD Biosiciences Clontech, CA, USA) and a plasmid encoding pdsFP593 fused to the amino terminus of FAT domain were used in this study. We call pdsFP593-FAT (focal adhesion targeting) domain, RFP (red fluorescent protein)-FAT domain. FAT domain is the 199 amino acid sequence from 854 to 1053 at the C terminus of FAK (Hildebrand et al. [9]). To observe actin structure and focal adhesions simultaneously, the plasmid vector encoding GFP-actin and RFP-FAT domain were co-transfected into cells planted on a 35-mm glass-base dish (Asahi Techno Glass, Chiba, Japan) by liposomal method. To observe microtubule structure, the plasmid vector encoding GFP-tubulin was transfected. Briefly, 1.0 μg of GFP-actin/2.0 μg of RFP-FAT domain or 1.0 μg of GFP-tubulin and 10 μl of PLUS reagent (Invitrogen, CA, USA) were incubated in 100 μl of OPTI-MEM (Invitrogen) for 15 min and then diluted with a solution of 7 μl of Lipofectamine (Invitrogen) and 100 μl OPTI-MEM, followed by incubation for 15 min at room temperature. This solution was diluted again with 0.8 ml of OPTI-MEM and added to cells at 40 - 50% confluence. After 4 - 5 h incubation at 37°C, the solution was replaced by 2 ml of DMEM and cells were then grown at 37°C for 24 - 48 h. In certain studies, cells were incubated with rhodamine-conjugated phalloidin (Molecular Probe, OR, USA) for actin filaments. Fluorescence images of cells were observed with an objective lens (PlanApo 60x TIRFM, Olympus, Tokyo, Japan) and captured with a digital CCD camera (C4742-95ER, Hamamatsu Photonics, Hamamatsu, Japan), under an inverted confocal laser scanning microscope (IX70, Olympus, Tokyo, Japan).

2.3 Fabrication of substrates with arrays of micropillars

Micropatterned substrates were created by the injection of polydimethylsiloxane (PDMS, Silpot 184W/C, Dow Corning Toray, Tokyo) into a silicon mold as described previously [4]. Fabrication process of arrays of mocropillars is shown in Fig. 1A. Firstly, a silicon wafer was spin-coated with a photoresist (a), and an i-line stepper was used to expose the wafer to ultraviolet light through a mask with

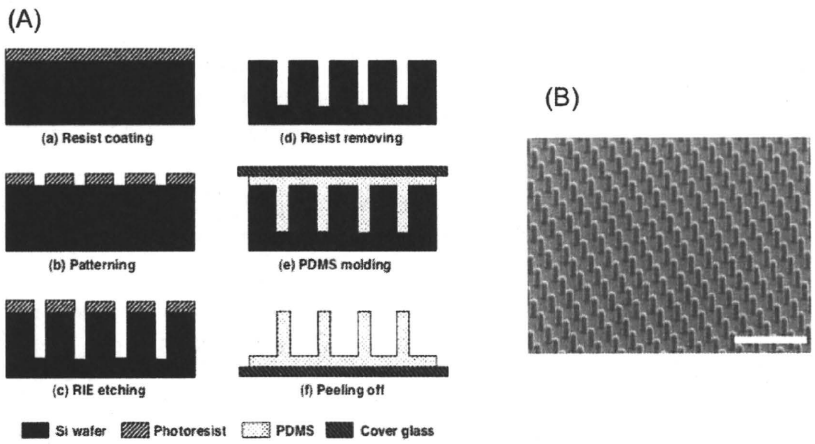

Fig. 1 Fabrication process of substrates with arrays of micropillars (A). Scanning electron microscope image of micropillars. (B). In (B), Bar = 30 μm.

pre-printed pattern followed by the development (b). The wafer was then etched using a reactive ion etching process (c). After removing the photoresist (d), the PDMS was poured over the etched substrates (e), degassed under vacuum, cured at 110°C for 1 h, and peeled off the substrates (f). A scanning electron microscope image of arrays of micropillars (ca. 3 μm in diameter, ca. 10 μm in height, and ca. 8 μm spacing) is shown in Fig. 1B. For experiments, the PDMS substrates were sterilized with UV light for 24 h and immersed in a 0.05 % gelatin solution to allow cells to attach to the top of micropillars. Cells were then incubated on the micropatterned substrates in the same culture medium for 24 h until experiments. It should be noted that since not only the top of the micropillars but also the side walls were coated with the gelatin, some cells went deep between the micropillars and attached to the side walls. Therefore, these cells were excluded from the analysis.

2.4 Determination of cellular traction forces

Traction force measurements were performed at room temperature. Cell spreading produced deflection of micropillars, showing subcellular distribution of tractions forces. Brightfield images of micropillars were captured before and after removing cells with a treatment of trypsin-EDTA. This treatment allows micropillars to return to the original position. Deflection of micropillars was thus measured by comparing these two brightfield images with an image analysis technique using the public domain NIH Image software version 1.62 (National Institute of Health, MD, USA). Traction forces F were then determined using the simple equation, $F = kx$, where k and x are the spring constant and the deflection of the micropillars, respectively. The spring constant was determined using a cross-calibration technique prior to experiments with a hydraulic micromanipulator (MMO-203, Narishige, Tokyo, Japan), ranging from 0.01 to 0.02 N/m. The force resolutions was 2.15 nN.

2.5 Disruption of microtubules

In order to know how microtubules contribute to traction forces, microtubules were disrupted with a treatment of 10 μg/ml nocodazole over 5 min. Changes in cytoskeletal structures and traction forces were studied before and after the disruption of microtubules.

2.6 Inhibition of signaling pathways of myosin light chain phosphorylation

Firstly, cells were treated with Phospho-Myosin-Light-Chain 2 (Thr 18/Ser 19) antibody (Cell Signaling Technology, MA, USA) to see if phosphorylation of myosin light chain could be induced after the disruption of microtubules. Then, blocking experiments of signaling pathways of myosin light chain phosphorylation were performed. For inhibition of Rho/Rho kinase (ROCK pathway), cells were treated with 20 μM Y27632 for 15 min prior to microtubules disruption.

2.7 Statistical analysis

Statistical comparisons were made using paired t-test. A value of $p < 0.05$ was considered significant in all analyses. Statistical data were shown as mean $\pm$ SD.

3. Results

Prior to traction force experiments, smooth muscle cells were transfected with GFP-actin and RFP-FAT domain, and then plated on the micropatterned substrates.

Typical fluorescence images of GFP-actin together with RFP-FAT domain in a cell and the superimposed images are shown in Figs. 2A, 2B and 2C, respectively. The cells spreaded on the substrates and showed clearly organized actin filament networks (Fig. 2A). Asymmetric distribution of FAT domain formed around micropillars (Fig. 2B), as pointed out by Chen et al. [10]. Stress fibers were anchored at the top of micropillars showing a close correlation with localization of FAT fomain (Fig. 2C). Estimated traction forces in the cell were correspondingly shown in Fig. 2D, showing that cell spreading on the substrates produced deflection of micropillars. Figure 2E shows a histogram of traction forces with 11.8 nN ± 12.9 nN (n =11).

Figure 3 shows a typical example of fluorescence images of GFP-tubulin, GFP-actin, and traction forces before and after the treatment with nocodazole. Filamentous structures of microtubules apparently started to disappear at 5 min after the treatment, preserving cell global shape, as typically shown in Figs. 3A and 3D (arrows). Even after the disruption of microtubules, actin filament structure seemed well maintained with no detectable change in the formation (Figs. 3B and 3E). Corresponding force vectors showed an increase in traction forces after the disruption of microtubules (Figs. 3C and 3F). Particularly, traction forces at the cell peripheries are likely to increase compared to the cell center. It has been confirmed

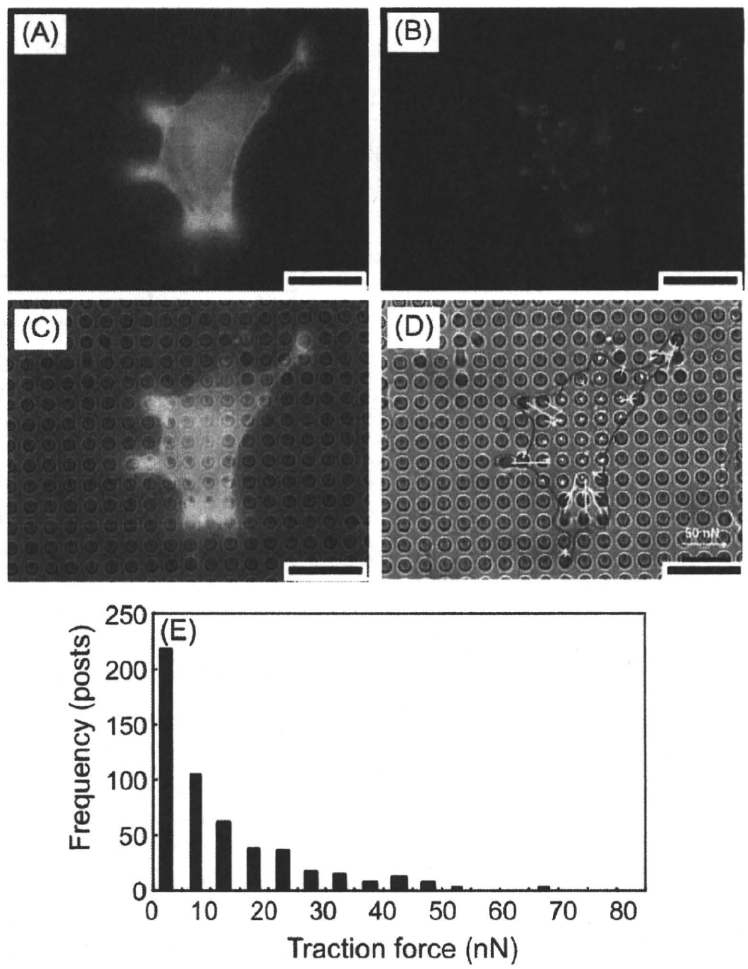

Fig. 2 Typical fluorescence images of GFP-actin (A), RFP-FAT domain (B) and overlay image of (A) and (B) (C), corresponding traction force vectors estimated by deflection of micropillars (D), and a histogram of traction forces (n =11) (E). In (D), arrows show direction and magnitude of traction forces. Bar = 30 μm.

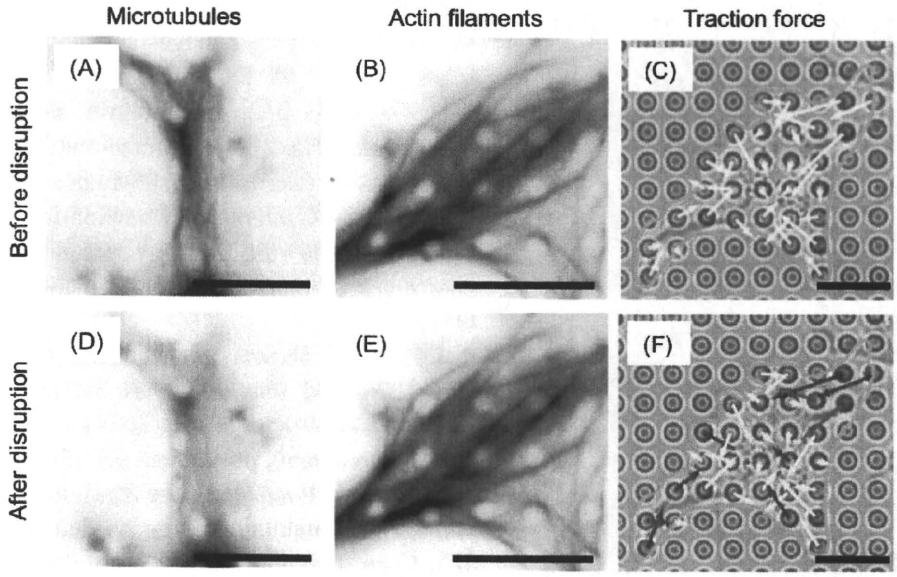

Fig. 3 Typical fluorescence images of GFP-tubulin (A, D) and GFP-actin (B, E) and corresponding traction force vectors (C, F) before and after treatment with nocodazole. In (F), red, yellow, and blue vectors indicate increased, unchanged, and decreased traction forces compared to (C). Traction forces significantly increased from 10.8 ± 8.2 nN (C) to 12.5 ± 8.3 nN (F). Bar = 20 μm.

Table 1 Change in traction forces before and after treatment with nocodazole (n = 5). $^{*}p < 0.01$ and $^{**}p < 0.05$ by paired t-test.

Cells	Microtubule disruption		Number of pillars
	Before	After	
#1	20.0 ± 17.6	27.0 ± 20.5*	43
#2	17.5 ± 14.9	19.8 ± 16.5**	79
#3	3.5 ± 3.1	6.5 ± 5.9*	37
#4	10.8 ± 8.2	12.5 ± 8.3*	31
#5	14.5 ± 15.4	17.0 ± 15.8*	88

that non-treated cells did not show any significant change in traction forces after 1 h. Please note that cells used for GFP-tubulin observation and GFP-actin observation were different due to technical reasons. Changes in traction forces before and after the treatment are summarized in Table 1 (n=5). The number of observed micropillars is also shown in the figure. After the disruption of microtubules, traction forces significantly increased for all the cells without change in the direction of traction forces, as typically shown in Figs. 3C and 3F. This tendency for traction forces and stress fiber formation did not change even after 1 h.

Figure 4 shows typical fluorescence images of rhodamine-phalloidin stained actin filament structure and phosphorylation of myosin light chain, which was observed for different cells before and after the disruption of microtubules. Even after the disruption of microtubules, stress fibers were still developed. Moreover, it was found that the disruption of microtubules could lead to phosphorylation of myosin light chain. Blocking experiments of signaling pathways of myosin light